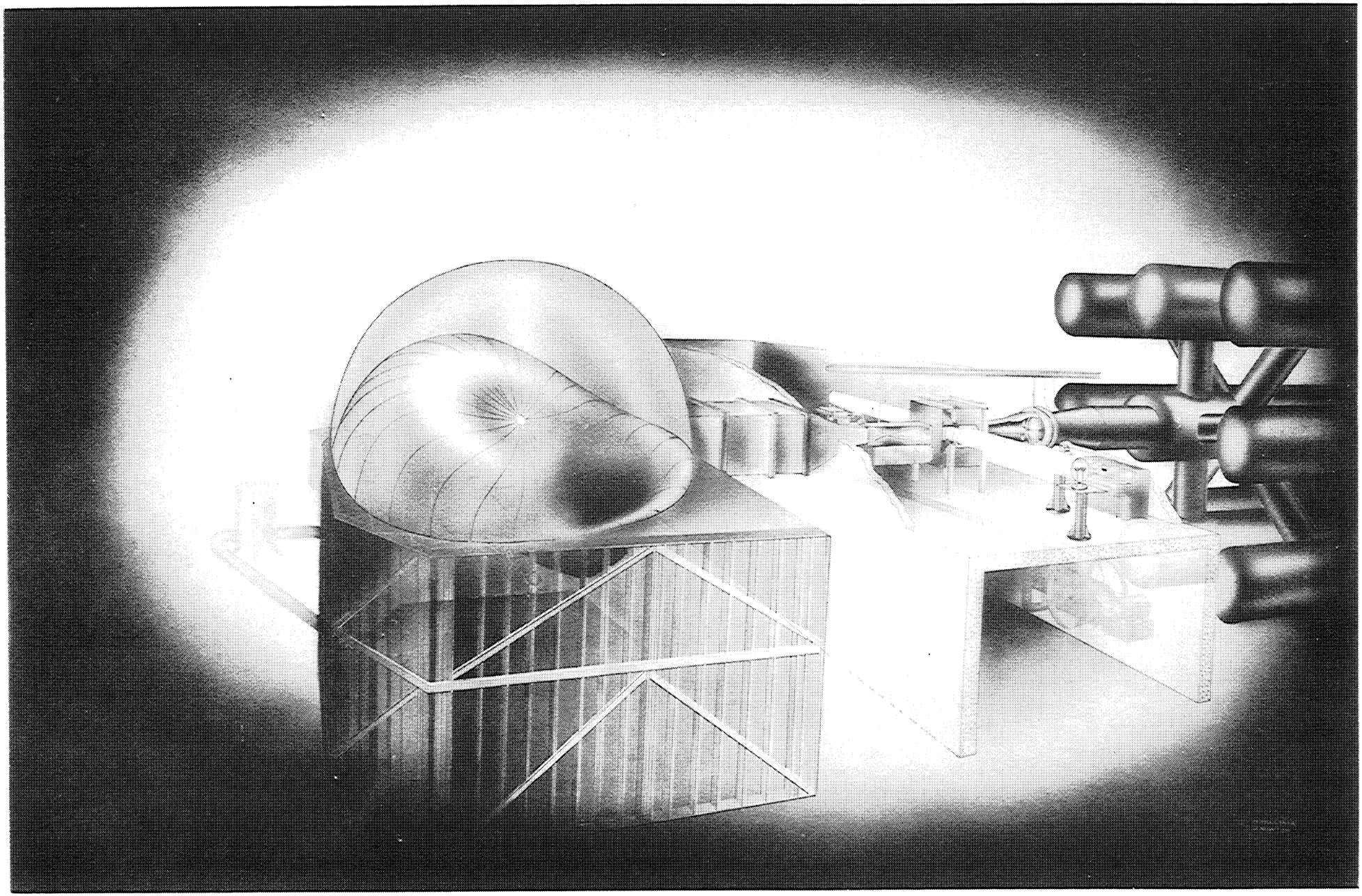

General Arrangement of 8 x 13-inch Supersonic Wind Tunnel Installation

ENGINEERING RESEARCH INSTITUTE
UNIVERSITY OF MICHIGAN
ANN ARBOR

CALIBRATION REPORT ON THE

UNIVERSITY OF MICHIGAN 8- BY 13-INCH SUPERSONIC WIND TUNNEL

PART V. AERODYNAMIC CALIBRATION AT NOMINAL MACH NUMBER OF 2.43

By

H. P. LIEPMAN

J. L. AMICK

T. H. REYNOLDS

WTM-248

(SECOND SUPPLEMENT TO UMM-36)

January, 1954

TABLE OF CONTENTS

LIST OF FIGURES

CALIBRATION REPORT ON THE

UNIVERSITY OF MICHIGAN 8- BY 13-INCH SUPERSONIC WIND TUNNEL

PART V. AERODYNAMIC CALIBRATION AT NOMINAL MACH NUMBER OF 2.43

SUMMARY

The nozzle blocks used in this calibration were designed for an outlet Mach number of 2.5 by a modified Nilson method without boundary-layer correction.

The average Mach number of the flow near the center of the test section was found experimentally to be 2.43. From 4 inches upstream to 4 inches downstream of the test-section center, the Mach number varies from 2.41 to 2.43 with local peaks of 2.45 due to disturbances from the window junctures. Flow conditions correspond to a Reynolds number of approximately 3.3×10^6 per foot.

Most of the flow angles measured in the test-section rhombus were within $\pm$ 0.2° except for local extremes, due to window disturbances, of +0.5° to -0.6° in angle of attack and from +0.9° to -0.9° in angle of yaw.

The stagnation pressure loss in the test section was found to be negligible. The allowable test dewpoint was estimated at -20°F.

INTRODUCTION

This report is the second supplement to the basic calibration report[1] of the 8- by 13-inch supersonic wind tunnel of the Department of Aeronautical

Engineering at the University of Michigan. Reference 1 described the tunnel and the associated equipment and presented the aerodynamic calibration of the flow at M = 1.90. The first supplement[2] to the basic report gave the calibration data at M = 2.84 and 1.44.

In the present report the aerodynamic calibration of the flow in the test section is presented for nozzle blocks designed to give an outlet Mach number of 2.5 by a modification of the Nilson method[3,4] without boundary-layer correction. The dimensions of the M = 2.5 nozzle blocks are listed in Table I. Frost's modification of the Nilson method consisted of the additional design requirement that the Mach-number gradient dM/dx be continuous throughout the nozzle.[3] This was accomplished by assuming a sinusoidal function for the

TABLE I
MACH-2.5 NOZZLE ORDINATES

X"	Y"	X"	Y"	X"	Y"
-13.445	7.500	5.651	3.049	30.183	6.381
-12.938	7.368	6.119	3.141	31.455	6.421
-12.445	7.046	6.586	3.238	32.714	6.451
-11.952	6.609	7.053	3.339	33.951	6.472
-11.459	6.129	7.519	3.444	35.159	6.486
-10.719	5.491	7.986	3.552	36.329	6.494
-10.111	5.066	8.453	3.662	37.455	6.498
- 9.447	4.659	8.921	3.774	38.529	6.500
- 8.735	4.277	9.389	3.887	39.545	6.500
		(I) 9.663			
- 7.978	3.924	9.858	4.000		
- 7.183	3.605	10.328	4.112		
- 6.355	3.324	10.800	4.222		
- 5.499	3.081	11.274	4.329		
- 4.619	2.879	11.750	4.433		
- 3.720	2.719	12.228	4.533		
- 2.805	2.599	12.794	4.645		
		(PML) 13.287			
- 1.879	2.518	13.798	4.826		
- 0.943	2.475	14.823	4.974		
T 0.000	2.465	15.871	5.151		
0.473	2.472	16.941	5.298		
0.946	2.487	18.034	5.438		
1.419	2.510	19.152	5.570		
1.891	2.540	20.295	5.694		
2.363	2.579	21.463	5.812		
2.835	2.625	22.655	5.922		
3.306	2.678	23.871	6.023		
3.776	2.739	25.108	6.116		
4.246	2.807	26.363	6.198		
4.715	2.881	27.630	6.270		
5.183	2.962	28.906	6.331		

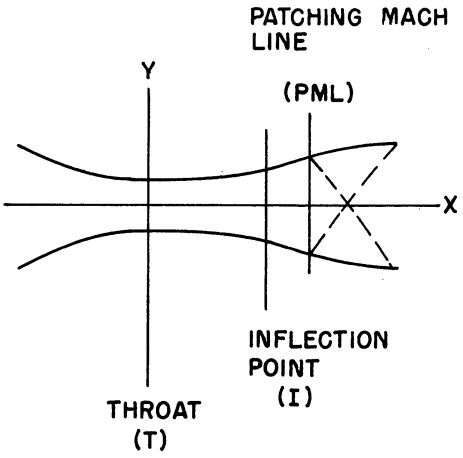

area parameter $\bar{h}$ along the centerline instead of Nilson's quadratic representation. Continuity of dM/dx also assures continuity in the curvature of the nozzle contour as shown in References 3 and 5.

Since most of the instrumentation and techniques used in this calibration have been adequately described in Reference 1, the experimental data will be presented without an extensive discussion of the methods, except in the case of flow-inclination measurements, which were obtained with a new probe.

MACH-NUMBER DISTRIBUTION

The Mach-number distribution was evaluated by means of static pressure orifices on the tunnel walls and by means of the five-prong total-head probe in the test section.[1] The measured static and total pressures were converted to Mach number with the assumption of isentropic flow, which is justified by the stagnation-pressure measurement presented later. Mercury manometry was used to measure the total pressures and static pressures upstream of station 40, while static pressures downstream of station 40 were measured by oil manometry. The specific gravity of the Meriam red oil used, compared with water at 39°F, was found by calibration against distilled water to be 0.839 at 72°F, decreasing by 0.00367 for each °F rise above 72°F. The standard deviation in measurements of the ratio of static pressure to barometric pressure by oil manometry was found to be 0.00015.

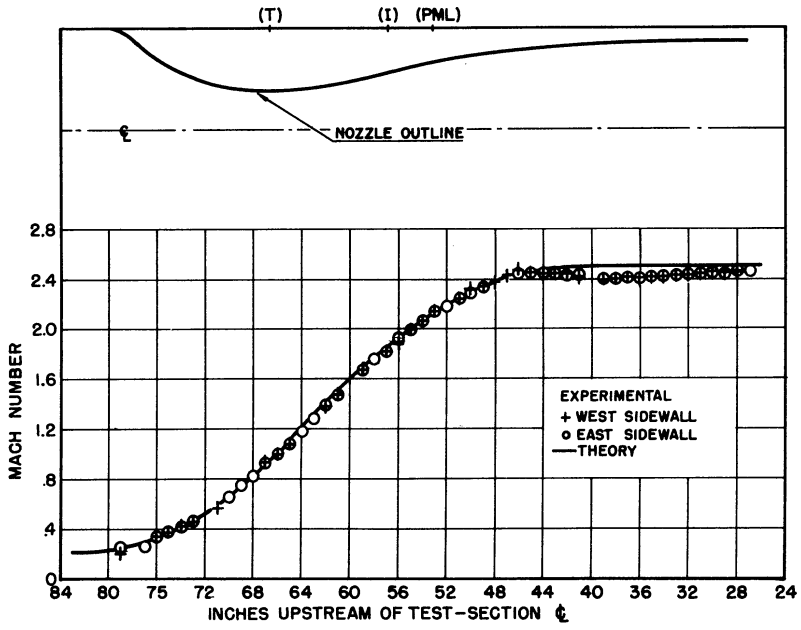

Fig. 1. Nozzle Outline and Mach-Number Distribution on Centerline of Nozzle Sidewalls

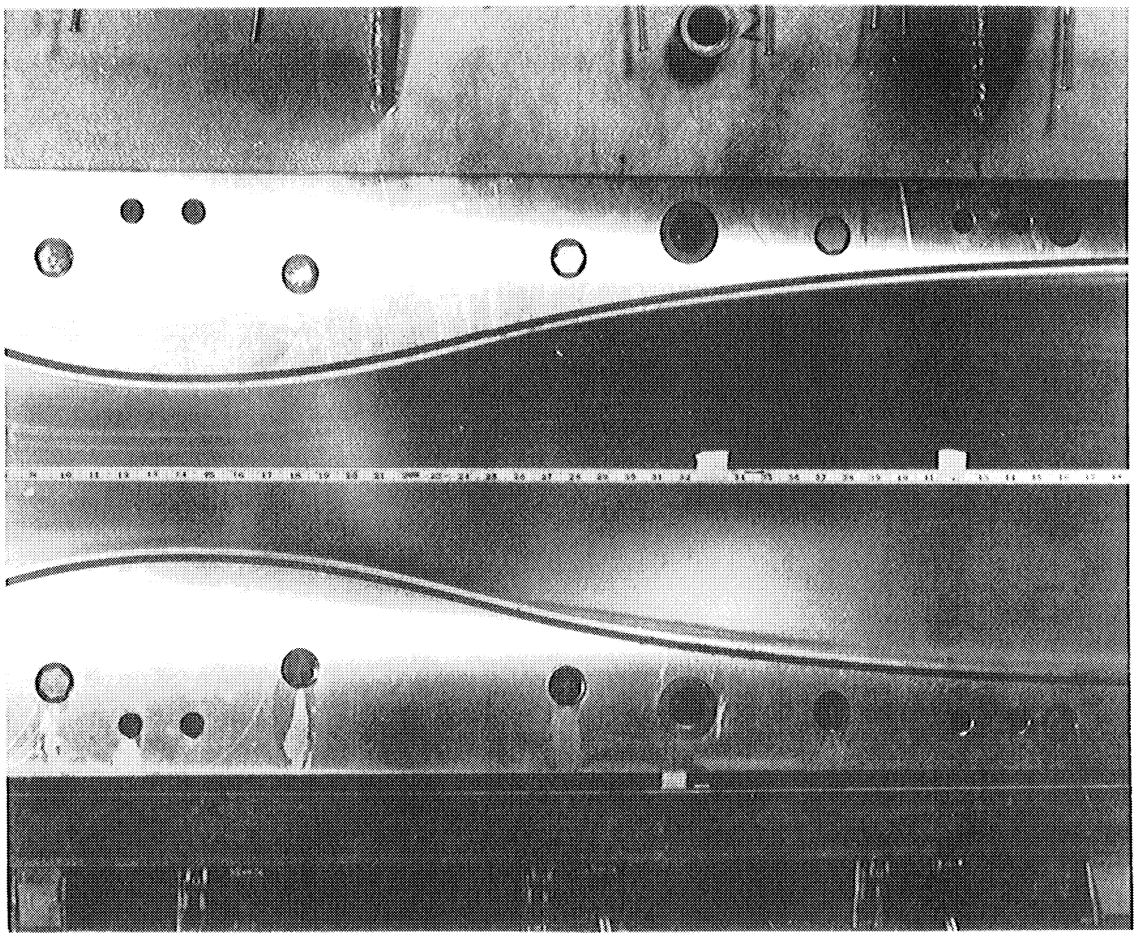

(a)

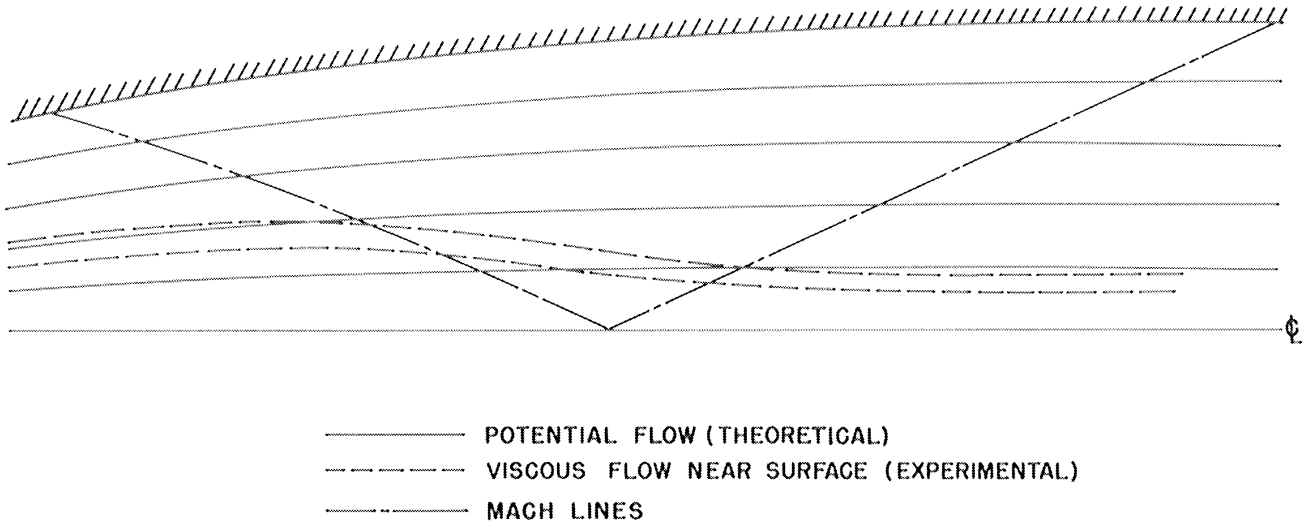

(b)

Fig. 2. Photograph of Oil Streaks on Nozzle Sidewall and Comparison with Theoretical Streamlines

Figure 1 compares the theoretical Mach-number distribution on the nozzle walls with experimental values. The agreement is good until the flow reaches a point about 20 inches downstream of the throat; beyond this point the experimental values are lower than the theoretical ones. It is believed that this deviation is due to boundary-layer thickening on the sidewalls. The vertical pressure gradients in the nozzle tend to create a boundary-layer flow from the top and bottom of the nozzle toward the sidewall centerlines. The effect is greatest above and below the intersection of the patching Mach line with the sidewall centerline, which is the upstream limit of the theoretical constant-Mach-number region. Visual evidence of this well-known phenomenon is shown in Fig. 2. Figure 2(a) shows oil streaks on the nozzle sidewalls, and Fig. 2(b) shows a comparison of these actual streamlines in the viscous layer near the wall with theoretical streamlines of the main (potential) flow. The maximum angular discrepancy between these streamlines is about 10°.

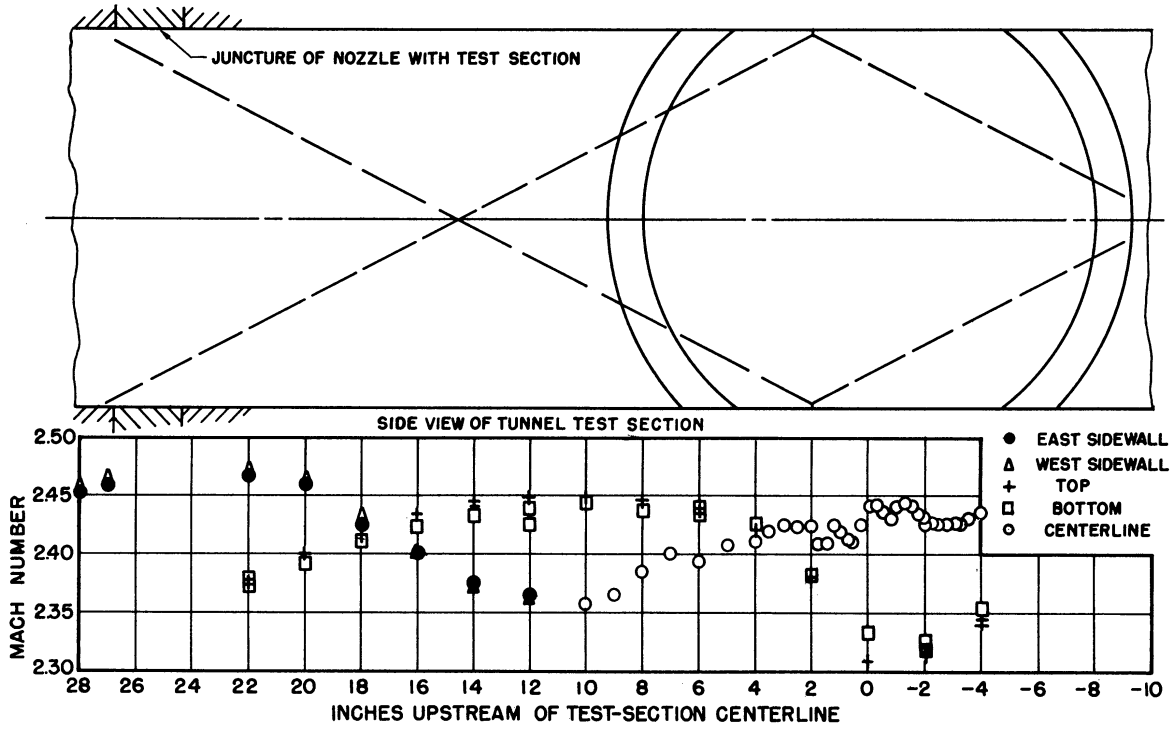

Fig. 3. Vertical Shock Pattern and Mach-Number Distribution in Test Section

The Mach-number distribution on the tunnel walls downstream of the nozzle exit and on the axial centerline in the test section is shown in Fig. 3, which is a sketch of the test section showing the location of the two principal observed shocks (see the schlieren photograph of Fig. 4) which appear to originate from the horizontal joints between the nozzle and the test section. The Mach-number distribution can be correlated with these shocks and their

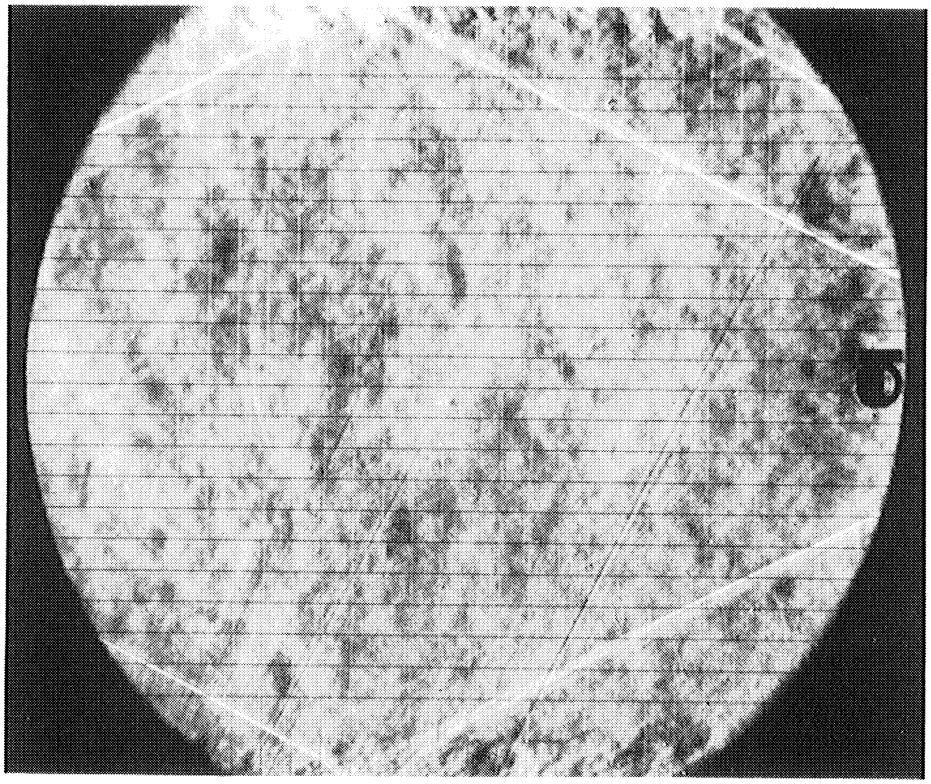

Fig. 4. Schlieren Photograph of Test Section at Mach 2.43 without Model

associated expansion regions. The decreases in Mach number from station 20 to station 12 on the east and west sides of the tunnel, and from station 6 to station 0 on the top and bottom of the tunnel, are due to the compression across the shocks. The increases in Mach number from station 22 to station 14 on the top and bottom of the tunnel, from station -2 to station -4 on the top and bottom of the tunnel, and from station 10 to station 4 along the centerline of the tunnel are due to the expansion regions behind the shocks. Superimposed on this pattern of Mach-number gradients is a general decline in Mach number due to the growth of the boundary layers on the parallel test-section walls.

The Mach-number distributions in the horizontal and vertical planes of the test section are shown in Figs. 5 and 6 respectively. The average Mach number of the flow at the center of the test section is 2.43. From 4 inches upstream to 4 inches downstream of the test-section center, the Mach numbers vary from 2.41 to 2.43 with local peaks up to 2.45. In the region from 4 to 10 inches upstream of the test-section center, the Mach numbers gradually decrease to 2.36.

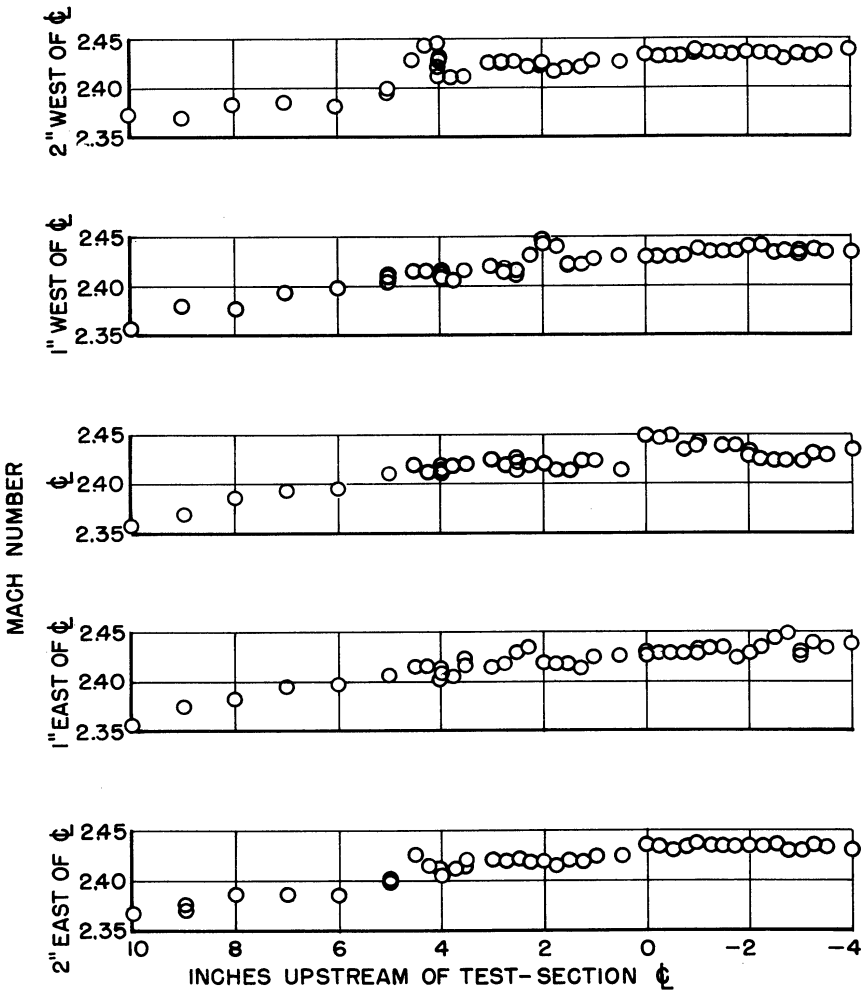

Fig. 5. Mach-Number Distribution in Horizontal Plane through the Test-Section Centerline

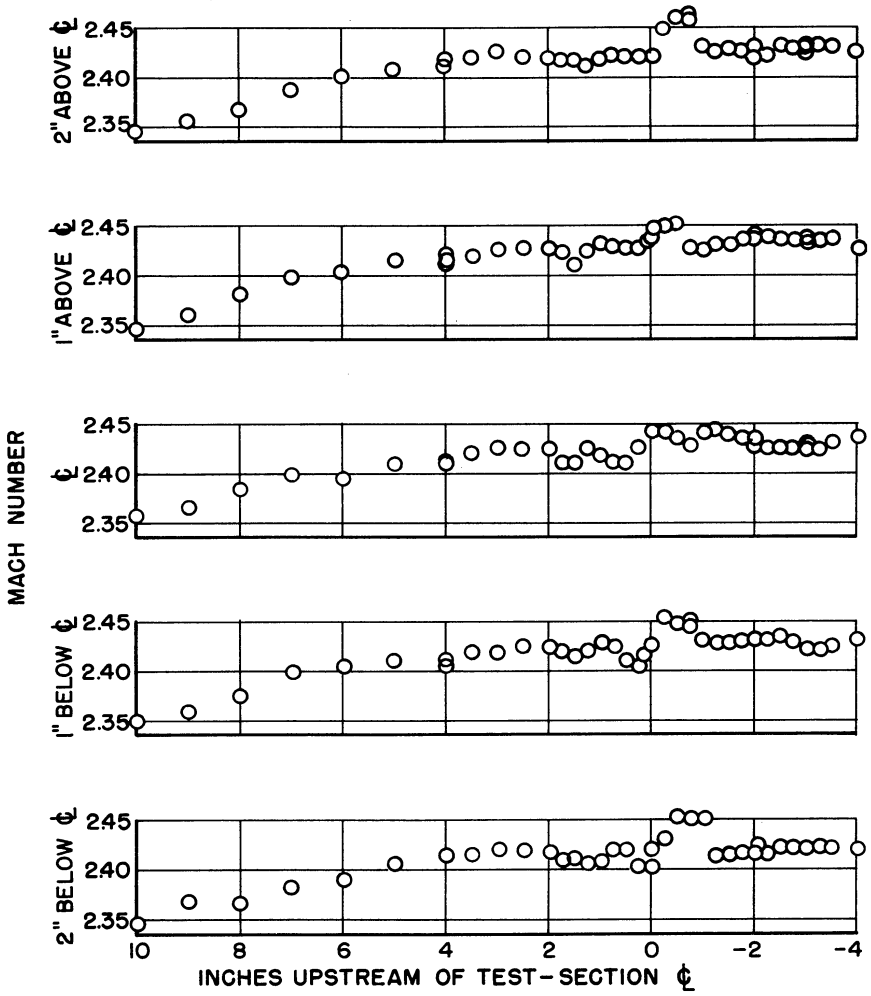

Fig. 6. Mach-Number Distribution in Vertical Plane through the Test-Section Centerline

A line drawn through the major local irregularities in the horizontal plane shows that the expansions and shock waves causing them probably originate from the window junctures. The probable path of these disturbances is indicated in Fig. 7, which also presents cross sections of the two sidewall-window junctures. The east wall is somewhat smoother than the west wall. The east wall has one 0.008-inch drop and one 0.004-inch drop, while the west wall has a 0.005-inch drop, a 0.004-inch rise, and then a 0.013-inch drop again. It would be possible to alleviate these irregularities somewhat, but to eliminate them altogether would be very difficult. These step heights are larger than those at the juncture of the nozzle with the test section, which are probably not greater than 0.002 inch.

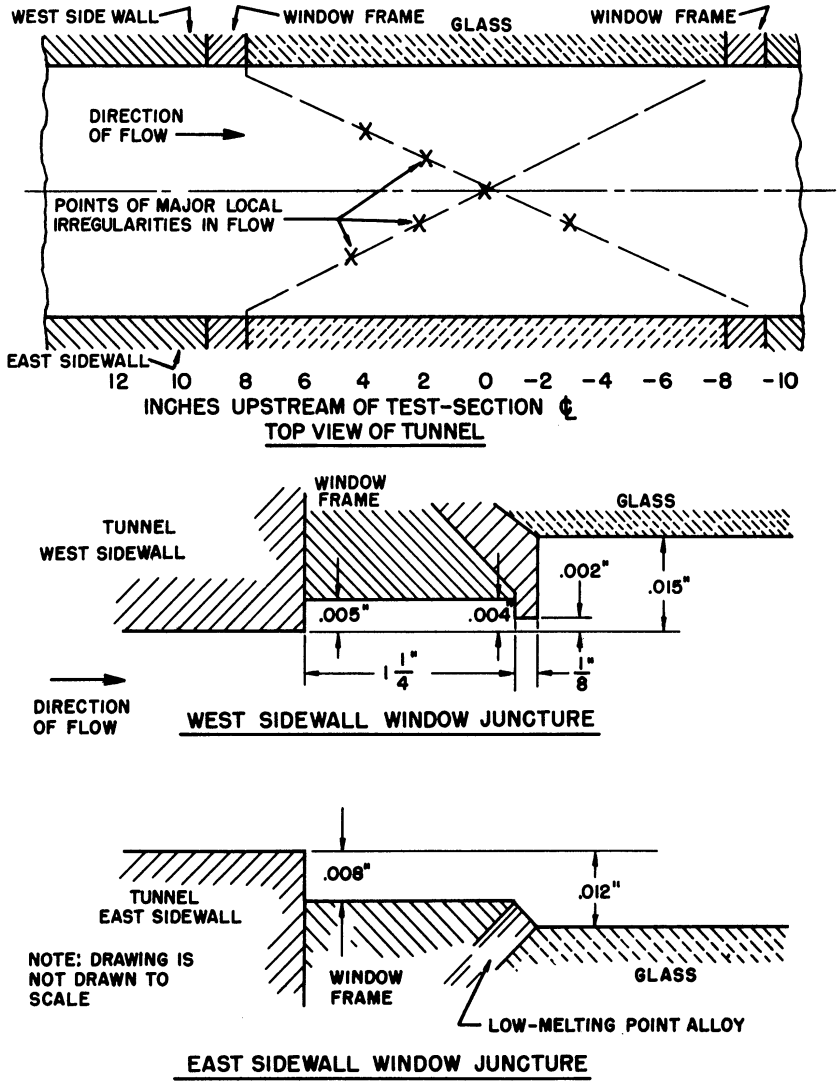

Fig. 7. Horizontal Shock Pattern in Test-Section and Sidewall-Window Junctures

FLOW INCLINATION

Instrumentation

The five-cone probe shown in Fig. 8 was used to measure the flow inclination. It is composed of five cones with total cone angles of 60°. The center cone has six equally spaced orifices; the four outer cones have four equally spaced orifices. These orifices have 0.025-inch diameters and are on 0.195-inch-diameter circles. The centers of the outer cones are 1-1/2 inches from the midpoint of the center cone at 90° intervals. The probe was mounted on the arc-sector strut of the wind tunnel.[1] The pressures at the orifices were measured on a manometer board using Meriam red oil.

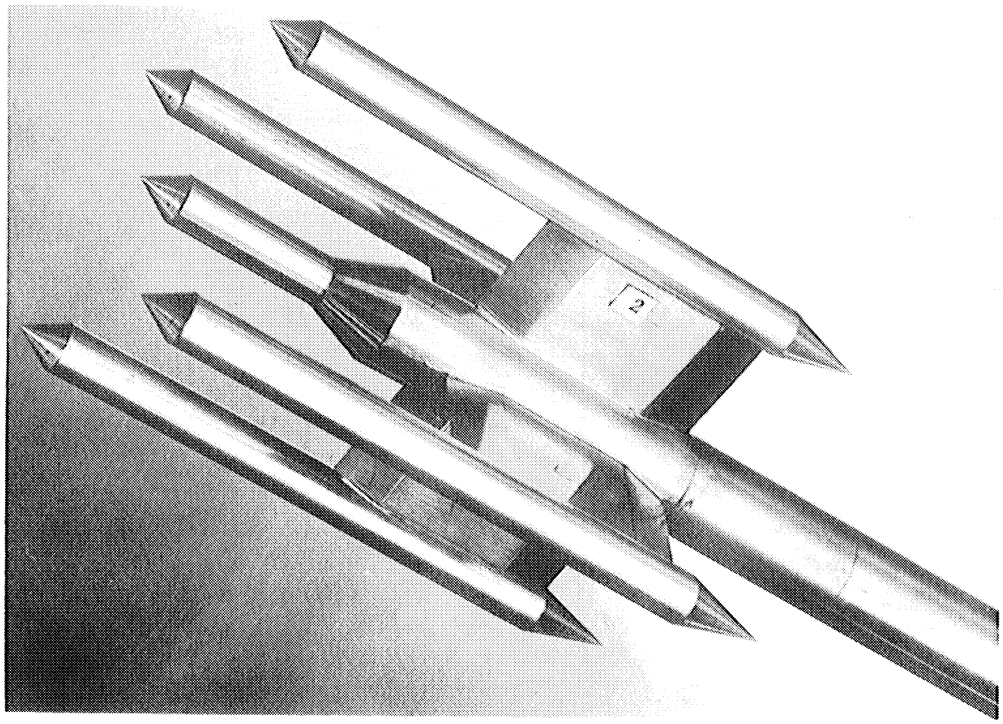

Fig. 8. Five-Cone Probe

Calibration of Instrument

In order to determine the sensitivity of the instrument to changes in flow direction, it was mounted so that the center and side cones were very near the axis of rotation of the strut. When the strut was revolved to an

angle of attack, the orifices of the center and side cones remained effectively fixed. For an angle of attack of 4°, the upper and lower cones moved approximately 0.1 inch from their positions at zero angle of attack.

By setting the instrument at various angles of attack in the flow, the rate of change of the pressure difference between the upper and lower orifices with the angle of attack was obtained. (The center cone has two orifices on the top and two orifices on the bottom. Here the sum of the pressures of the upper orifices was subtracted from the sum of the pressures of the lower orifices.) At the same time the effect of angle of attack on the pressure difference between left and right orifices on each cone was measured. This latter effect was small and would theoretically be zero if the side orifices and the flow were perfectly symmetrical.

Typical cone-sensitivity calibration plots obtained by this procedure are shown in Figs. 9 and 10. Figure 9 shows the sensitivity of the top and bottom orifices of one of the cones to flow inclination in the vertical plane, along with the theoretical sensitivity given by Reference 6. Figure 10 shows

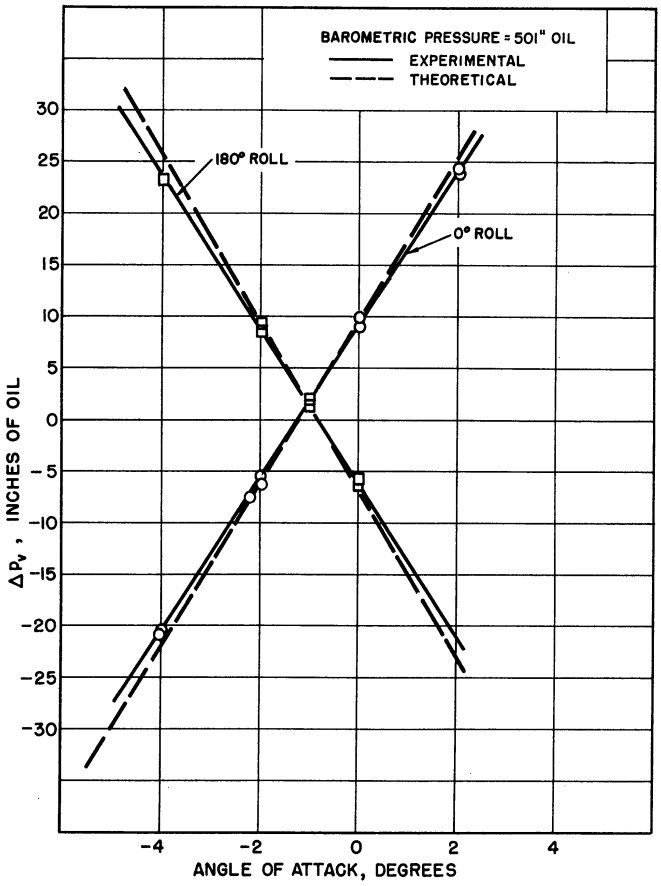

Fig. 9. Sensitivity of Top and Bottom Orifices to Vertical Flow Inclination

the interaction of vertical flow inclination with side orifices, which are intended to measure only flow angles in a horizontal plane. (The angles of attack shown in these figures are measured from an arbitrary fixed reference.)

Since the circular arc strut provides only the angle-of-attack variation, it was necessary to rotate the instrument 90° about its axis to determine the sensitivity of the side orifices to changes of flow angle in their own plane. The procedure was the same as that for the top and bottom orifices and was repeated with the instrument inverted in order to obtain a check on cone alignment with the sting.

The interaction between the effects of flow angles in the vertical and horizontal planes was eliminated by solving two simultaneous equations,

$$\Delta p_H = K_1\alpha + K_2\beta \qquad (1)$$

and

$$\Delta p_V = K_3\alpha + K_4\beta \ . \qquad (2)$$

In these equations α and β are the flow angles in the vertical and horizontal planes, respectively; K_1, K_2, K_3, and K_4 are the calibration constants of one

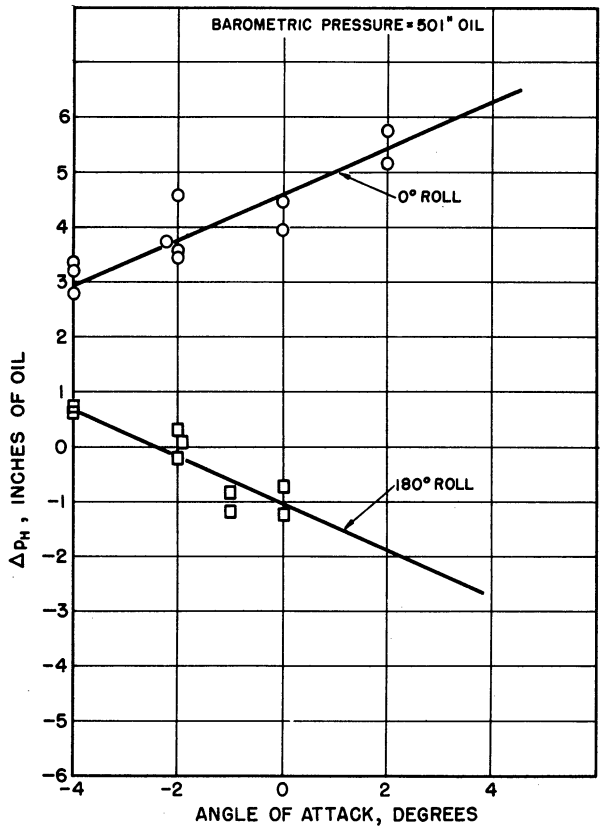

Fig. 10. Interaction of Vertical Flow Inclination with Side Orifices

of the cones; and Δp_H and Δp_V are the differences in pressure between two orifices in the horizontal and vertical planes, respectively. In general, K_1 and K_4 are small compared to K_2 and K_3, and would be zero if the orifices were perfectly aligned in the horizontal and vertical planes.

Solving equations (1) and (2) for α and β, we get

$$\alpha = c_1 \Delta p_V - c_2 \Delta p_H \qquad (3)$$

and

$$\beta = c_3 \Delta p_V - c_4 \Delta p_H \ , \qquad (4)$$

where

$$c_1 = \frac{K_2}{K_2K_3 - K_4K_1} \ , \qquad c_2 = \frac{K_4}{K_2K_3 - K_4K_1} \ ,$$

$$c_3 = \frac{K_1}{K_1K_4 - K_3K_2} \ , \text{ and } \qquad c_4 = \frac{K_3}{K_1K_4 - K_3K_2} \ .$$

Equations for α and β are thus obtained for each of the five cones.

Tests and Corrections

The flow was surveyed from 8 inches ahead of to 2-1/2 inches behind the test-section center at intervals of 1/2 inch or 1 inch. For these runs the arc-sector strut remained at a fixed angle of attack.

The sting was measured before each run by a height gage to get its angle of attack and angle of yaw with respect to the tunnel floor and the west wall. The distance between the front and rear measurements was 20.3 inches for the angle-of-attack and 16.8 inches for most of the angle-of-yaw measurements. From the scatter of the measured values of sting misalignment, it is deduced that the probable maximum error in these measurements was $\pm 0.03°$.

The measured pressure differences between opposing orifices of each cone were converted to the indicated values of α and β by means of equations similar to (3) and (4). Corrections were then applied to α and β for cone misalignment from the sting and the sting misalignment in the tunnel. The cone-misalignment correction was obtained by averaging the flow through the test section after the sting-misalignment correction had been applied. Assuming that the average through the length of the surveyed region of the flow angles indicated by each cone would be zero, any deviation of this average from zero was attributed to cone misalignment. This was checked by measuring

the difference between the 0° roll calibration and the 180° roll calibration at zero angle of attack. The two methods checked in the case of the center cone. The four outer cones could not be checked in this manner, since they change position when the probe is rotated 180°. The average cone misalignment was 0.3°.

The flow-angle measurements were found to be repeatable to within ±0.05°.

Results

The flow angles obtained are shown in Figs. 11 and 12. If the flow-angle deviations due to window disturbances are not considered, most of the remaining flow angles fall within the range of ±0.2°. The extremes due to window effects are from +0.5° to -0.6° for the vertical plane and from +0.9° to -0.9° for the horizontal plane. In addition, unexplained flow deviations of about ±0.5° exist about 7 inches ahead of and 2 inches behind the test-section center. The flow angles near shock waves are not expected to be very accurate because of interference between cone and shock wave.

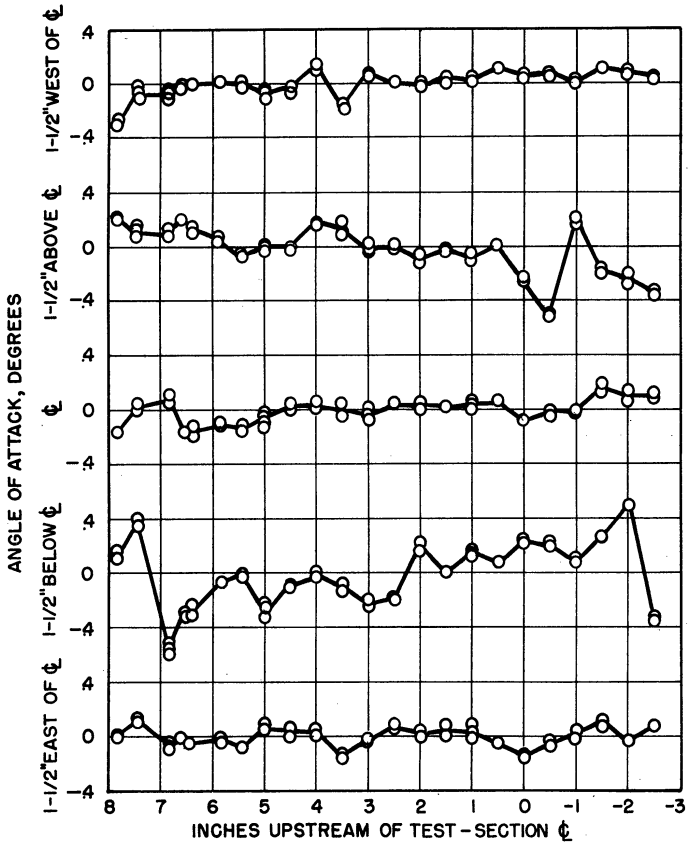

Fig. 11. Vertical Flow Inclination

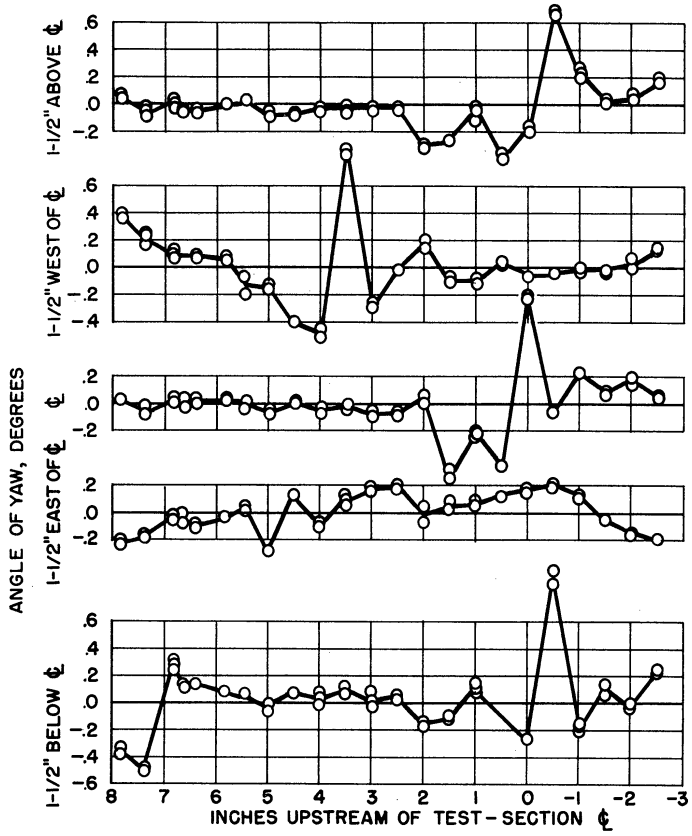

Fig. 12. Horizontal Flow Inclination

INFLUENCE OF DEWPOINT

The effect of dewpoint on static pressures 2.5 inches upstream of the test-section centerline was measured by means of the single static needle described in Reference 1. The colorless fluid butyl phthalate, whose specific gravity is 1.034 at 80°F, was used in the U-tube. The dewpoint effect on the total pressure at the same station was measured with the total-head rake.

Figures 13 and 14 respectively show the influence of dewpoint on the static-pressure ratio p_s/p_b and the total-head probe ratio p_o'/p_b, 2.5 inches upstream of the test-section center. The change in dewpoint only slightly affects the total-head measurements, because the shock from the total-head probe gets weaker as the condensation shock gets stronger. As the dewpoint decreases from +40°F to -40°F the static-pressure ratio decreases from 0.070 to 0.0655. For dewpoints below -20°F the increase in static pressure due to condensation is masked in the experimental scatter of static-pressure measurements. Consequently, the allowable test dewpoint can be considered to be -20°F.

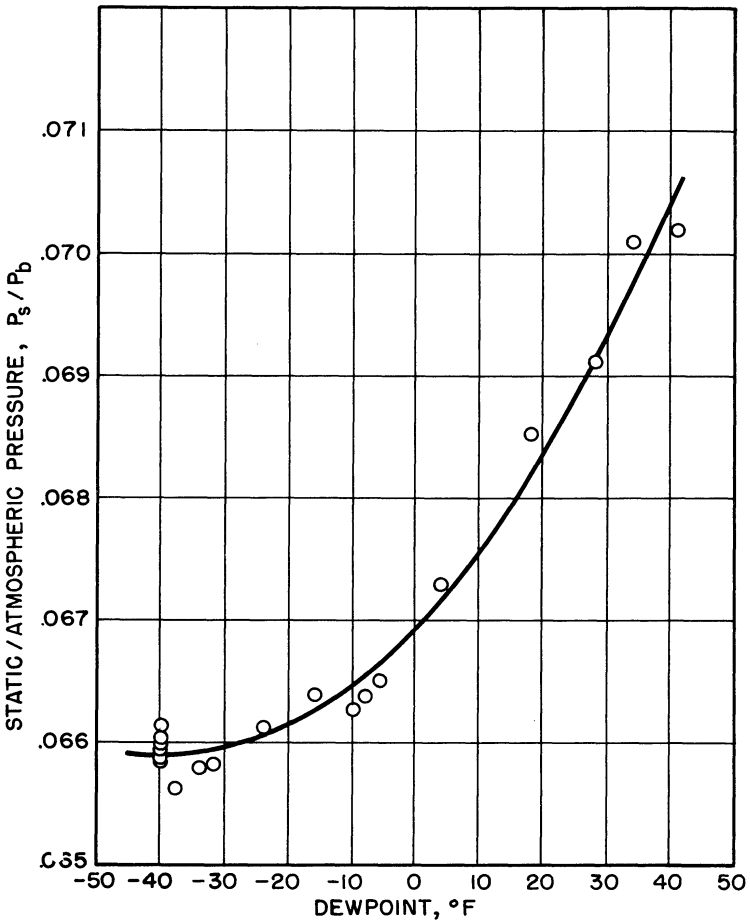

Fig. 13. Influence of Humidity on Static Pressure 2.5 Inches Upstream of Test-Section Centerline

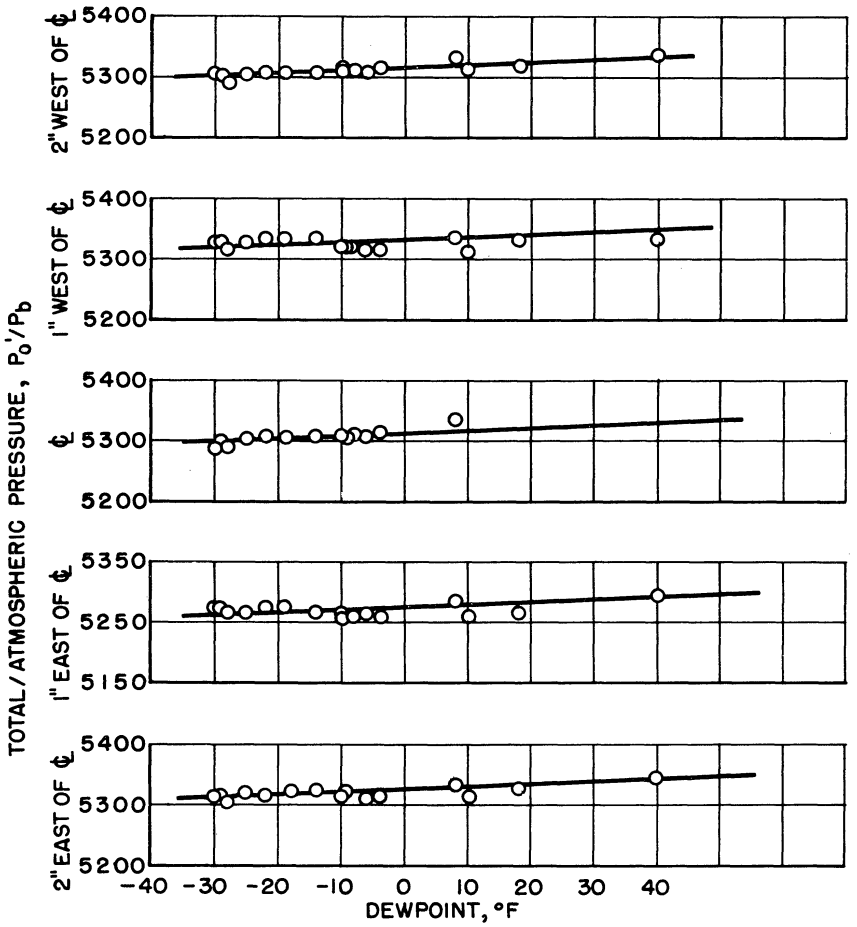

Fig. 14. Influence of Humidity on Total Pressure 2.5 Inches Upstream of Test-Section Centerline

STAGNATION PRESSURE IN THE TEST SECTION

Comparison of the static and total pressures measured 2.5 inches upstream of the test-section center at dewpoints below -20°F gives values of the stagnation pressure loss through the nozzle varying between 1.0 and -0.8 percent, with an average value of 0.1 percent. Thus it can be said that there is no loss in stagnation pressure within the measuring accuracy of the equipment. The stagnation pressure loss through the turbulence screens was found to be 0.1 percent, which is small enough to be neglected.

BLOCKING AND RUN TIME

No tests were made of the blocking characteristics of the Mach-2.43 flow. However, blocking was tested at Mach 1.90, where model size is more critical.[1]

Run time was not investigated for the Mach-2.43 flow.

REFERENCES

1. Culbertson, P.E., "Calibration Report on the University of Michigan Supersonic Wind Tunnel, Parts I and II", UMM-26, Univ. of Mich., Eng. Res. Inst., November, 1949.

2. Culbertson, P.E., "Calibration Report on the University of Michigan Supersonic Wind Tunnel, Parts III and IV", WTM-213, Univ. of Mich., Eng. Res. Inst., June, 1952.

3. Frost, R.C., "Nozzle Design Considerations", WTM-188, Univ. of Mich., Eng. Res. Inst., October, 1950.

4. Nilson, E., "Design of an Inlet for a Two-Dimensional Supersonic Nozzle", Meteor Report, UAC-13, December, 1947.

5. Frost, R.C., and Liepman, H.P., "Supersonic Nozzles with Continuous Wall Curvature", Journ. Aero. Sci., 19, No. 10, 716 (October, 1952).

6. Kopal, Zdenek, "Tables of Supersonic Flow Around Yawing Cones", Mass. Inst. of Tech., June, 1947.